INTERNATIONAL JOURNAL of RENEWABLE ENERGY RESEARCH
A. K. Biswas et al., *Vol.8, No.1, March, 2018*

The Photocurrent and Spectral Response of a Proposed p^+p n n^+ Silicon Solar Cell

Ashim Kumar Biswas*‡, Sayantan Biswas*, Amitabha Sinha*

*Department of Physics, University of Kalyani, Kalyani-741235, West Bengal, India.

(kumarashimbiswas@gmail.com, sayan.solar@gmail.com, asinha333@gmail.com)

‡Corresponding Author; A. K. Biswas, Department of Physics, Nabadwip Vidyasagar College, Nabadwip, Nadia - 741302, West Bengal, India, Tel: + 91 9531631423, kumarashimbiswas@gmail.com

Received: 24.05.2017 Accepted:31.05.2017

Abstract-In this paper an analytical work has been carried out on a p^+ p n n^+ structure photovoltaic cell in which a low- high junction is present in the front as well as the rear side of the device. The expressions for photocurrent and spectral response of this solar cell structure have been obtained and their variations with different device parameters and wavelength of incident light have been shown graphically. It is observed from theoretical considerations that this structure gives improved performance over previous silicon solar cell structures.

Keywords Si solar cell; high-low junction; front surface field; photocurrent; spectral response.

1. Introduction

After the first silicon solar cell was developed [1], lot of research work have been made to improve the performance of these cells, the most recent one being quantum dot and quantum well solar cells [2-9]. Now a day solar cells have become a strong contender for generation of energy. Their applications in various aspect, and analylitycal and experimental studies have been reported by researchers [10-13]. The first major improvement in the efficiency of a conventional solar cell was obtained by incorporating a low-high junction at its back which gave the n^+ p p^+ structure [14]. This p p^+ junction gave rise to a back surface field and the device was called a back surface field (BSF) solar cell. Theoretical studies on these BSF solar cells were performed and the improvement in the efficiency was attributed to the reduction in the back surface recombination in these cells [15, 16]. It was then suggested that a low-high junction may be incorporated at the front surface of the solar cell to give rise to n^+ n p structure [17-19]. This high-low junction emitter structure gave increased open-circuit voltage and short-circuit current. Further theoretical investigations on the front-surface -field (FSF) solar cells were carried out and it was shown that a low-high junction had the significant role to collect light generated current [20]. The role and function of front- surface-field on an n^+ n p GaAs solar cell has been reported recently [21] in which a high-low junction factor F_{h-l} has been introduced. F_{h-l} determines the effective carrier collection of the low-high junction. Dark current generating in a solar cell has an important contribution in calculating the overall efficiency of such device. Its experimental and analytical studies has been discussed in [22, 23] based on different cell parameters including doping effects. In our present work we have assumed a p^+ p n n^+ solar cell structure that has low-high junction at both the front and the rear surfaces giving rise to front surface field (FSF) as well as back surface field (BSF). A complete analytical study for this proposed new structure has been carried out.

2. Analysis

Silicon solar cell considered in this study is highlighted in Fig. 1. The front and rear parts of this p^+ p n n^+ structure are formed with a p^+ p and an n n^+ low-high junctions respectively. The thicknesses of the quasi-neutral p^+, p, n and n^+ layers considered for this cell are W_{p^+}, W_p, W_n and W_{n^+} respectively. W_a, W_d and W_b are the widths of the depletion regions at the respective junctions.

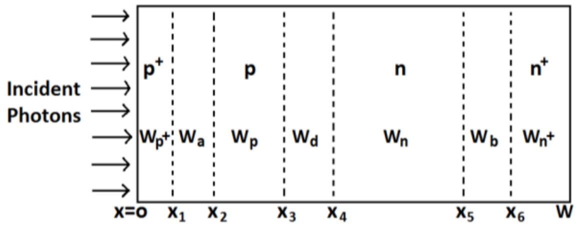

Fig. 1. The p^+ p n n^+ solar cell structure.

As shown in the Fig. 1,

$x_1 = W_{p^+}, x_2 = W_{p^+} + W_a,\ x_3 = W_{p^+} + W_a + W_p,$

$x_4 = W_{p^+} + W_a + W_p + W_d,$

$x_5 = W_{p^+} + W_a + W_p + W_d + W_n$

$and\ \ x_6 = W_{p^+} + W_a + W_p + W_d + W_n + W_b.$

The photocurrent contribution from each layer of the solar cell and also from the depletion regions may be found out by solving the current density and the continuity equations with special boundary conditions [21, 24].

The required boundary conditions for p^+ region are

$$D_n^+ \frac{d(\Delta n)_{p^+}}{dx} = S_n (\Delta n)_{p^+} \qquad at\ x = 0 \qquad (1)$$

$$(\Delta n)_{p^+} = \Delta n_o \qquad at\ x = x_1 \qquad (2)$$

where Δn_o denotes the excess electron density at high-low junction.

Solution of the electron continuity equation along with the current density equation in using the above two boundary conditions gives the following expression of excess electron density at p^+ region.

$$(\Delta n)_{p^+} = \left(\frac{\Gamma L_n^+}{qD_n^+}\right)$$

$$\times \left[\frac{\left(\frac{S_n L_n^+}{D_n^+} + \alpha L_n^+\right) sinh\left(\frac{x_1 - x}{L_n^+}\right) + \left(\frac{S_n L_n^+}{D_n^+} sinh\left(\frac{x}{L_n^+}\right) + cosh\left(\frac{x}{L_n^+}\right)\right)\left(exp(-\alpha x_1) + \left(\frac{\Delta n_o}{\Gamma L_n^+}\right) qD_n^+\right)}{\frac{S_n L_n^+}{D_n^+} sinh\left(\frac{x_1}{L_n^+}\right) + cosh\left(\frac{x_1}{L_n^+}\right)} - exp(-\alpha x) \right] \qquad (3)$$

$$with\ \ \Gamma = \frac{qF(1-R)\alpha L_n^+}{(\alpha^2 L_n^{+^2} - 1)}$$

where α is the absorption coefficient of the material.

The expression of the photocurrent density generated in p^+ layer and collected at $x_1 (= W_{p^+})$ is seen as follows

$$J_{n,x_1}^+(\lambda) =$$

$$-\Gamma \left[\frac{\left(\frac{S_n L_n^+}{D_n^+} + \alpha L_n^+\right) - \left(\frac{S_n L_n^+}{D_n^+} cosh\left(\frac{W_{p^+}}{L_n^+}\right) + sinh\left(\frac{W_{p^+}}{L_n^+}\right)\right)\left(exp(-\alpha W_{p^+}) + \left(\frac{\Delta n_o}{\Gamma L_n^+}\right) qD_n^+\right)}{\frac{S_n L_n^+}{D_n^+} sinh\left(\frac{W_{p^+}}{L_n^+}\right) + cosh\left(\frac{W_{p^+}}{L_n^+}\right)} - \alpha L_n^+ exp(-\alpha W_{p^+}) \right] \qquad (4)$$

where λ is the wavelength of incident light.

If $\Delta n_o = 0$, then $J_{n,x_1}^+(\lambda) = J_{n,x_1}^o(\lambda)$, the collected photocurrent at x_1 in the case of a conventional p-n junction cell. Imposing this condition in equation (4) the expression for $J_{n,x_1}^o(\lambda)$ is obtained as

$$J_{n,x_1}^o(\lambda) = -\Gamma \left[\frac{\left(\frac{S_n L_n^+}{D_n^+} + \alpha L_n^+\right) - \left(\frac{S_n L_n^+}{D_n^+} cosh\left(\frac{W_{p^+}}{L_n^+}\right) + sinh\left(\frac{W_{p^+}}{L_n^+}\right)\right) exp(-\alpha W_{p^+})}{\frac{S_n L_n^+}{D_n^+} sinh\left(\frac{W_{p^+}}{L_n^+}\right) + cosh\left(\frac{W_{p^+}}{L_n^+}\right)} - \alpha L_n^+ exp(-\alpha W_{p^+}) \right] \qquad (5)$$

Now, Substitution of equation (5) in equation (4) gives the following form of the photocurrent density.

$$J^{+}_{n,x_1}(\lambda) = J^{0}_{n,x_1}(\lambda) + \Gamma\left[\frac{\left(\frac{\Delta n_0}{\Gamma L_n^+}\right) q D_n^+ \left[\frac{S_n L_n^+}{D_n^+}\cosh\left(\frac{W_{p^+}}{L_n^+}\right) + \sinh\left(\frac{W_{p^+}}{L_n^+}\right)\right]}{\frac{S_n L_n^+}{D_n^+}\sinh\left(\frac{W_{p^+}}{L_n^+}\right) + \cosh\left(\frac{W_{p^+}}{L_n^+}\right)}\right] \qquad (6)$$

Due to presence of the high-low junction, surface recombination velocities in p^+ and p regions may be modified as effective surface recombination velocities S_{e,pp^+} and S_{e,p^+p} as suggested by Dai et al [20]. The high-low factor of low-high junction has been defined by the relation [21].

$$F_{h-l} = \frac{1}{1 + \left(\frac{S_{e,pp^+}}{S_{e,p^+p}}\right)\left(\frac{N^+_{aeff}}{N_{aeff}}\right)} \qquad (7)$$

The expression of the photocurrent, which is collected by the p-n junction at x_3, may be written as [21] with a correction factor

$$J^{+}_{n,x_3}(\lambda) = J^{0}_{n,x_1}(\lambda) F_{h-l}\,\mathrm{sech}\left(\frac{W_p}{L_n}\right) \qquad (8)$$

The photocurrent density collected at x_3 from the depletion layer of the low-high junction is given by the following equation [21].

$$J_{W_a,x_3}(\lambda) = qF(1-R)\,e^{-\alpha W_{p^+}}\left(1 - e^{-\alpha W_a}\right)\mathrm{sech}\left(\frac{W_p}{L_n}\right) \qquad (9)$$

where W_a is the thickness of depletion layer of the low-high junction.

Assuming the space charge region to be entirely spread into lightly doped region, its thickness W_a has been calculated using the expression discussed in [25].

Similarly, photocurrent contributions from p, n and depletion region of the p-n junction may be evaluated. With reference to the present structure of the solar cell and following [26, 27], the expressions of photocurrent collected from the p-region, n-region and the depletion layer are respectively given by

$$J_n(\lambda) = \left[\frac{qF(1-R)\alpha L_n}{\alpha^2 L_n^2 - 1}\right] \times \exp\{-\alpha(W_{p^+} + W_a)\}$$
$$\times\left[\frac{\left(\frac{S_{e,pp^+}L_n}{D_n} + \alpha L_n\right) - \left\{\frac{S_{e,pp^+}L_n}{D_n}\cosh\left(\frac{W_p}{L_n}\right) + \sinh\left(\frac{W_p}{L_n}\right)\right\}\exp(-\alpha W_p)}{\frac{S_{e,pp^+}L_n}{D_n}\sinh\left(\frac{W_p}{L_n}\right) + \cosh\left(\frac{W_p}{L_n}\right)} - \alpha L_n \exp(-\alpha W_p)\right] \qquad (10)$$

$$J_p(\lambda) = \left[\frac{qF(1-R)\alpha L_p}{\alpha^2 L_p^2 - 1}\right]$$
$$\times \exp\{-\alpha(W_{p^+} + W_a + W_p + W_d)\} \times \left[\alpha L_p - \frac{\left(\frac{S_{e,nn^+}L_p}{D_p}\right)\left[\cosh\left(\frac{W_n}{L_p}\right) - \exp(-\alpha W_n)\right] + \alpha L_p \exp(-\alpha W_n)}{\frac{S_{e,nn^+}L_p}{D_p}\sinh\left(\frac{W_n}{L_p}\right) + \cosh\left(\frac{W_n}{L_p}\right)}\right] \qquad (11)$$

and

$$J_{W_d}(\lambda) = qF(1-R)\exp\{-\alpha(W_{p^+} + W_a + W_p)\}\left(1 - e^{-\alpha W_d}\right)\mathrm{sech}\left(\frac{W_p}{L_n}\right) \qquad (12)$$

where S_{e,nn^+} is the effective recombination velocity of hole in n region due to the effect of n^+ region, and width of the depletion region formed between p and n layers has been calculated as [28].

Since n- n^+ low-high junction is present at the back side of the device, some currents are also generated in n^+ and n- n^+ space charge regions. Using similar boundary conditions as the calculation of photocurrent from front p^+ and p- p^+ high-low junction space charge regions, we can obtain the expressions for the photocurrents $J^{+}_{p,x_4}(\lambda)$ and $J_{W_b,x_4}(\lambda)$ collected from n^+ and n- n^+ high-low junction depletion regions.

Thus, the spectral response (SR) of the proposed p^+p n n^+ silicon device is given by the sum of the contributions from each layer of the cell including the contributions from all the depletion regions.

$$SR(\lambda) = \frac{J_{n,x_3}^{+}(\lambda) + J_{W_a,x_3}(\lambda) + J_n(\lambda) + J_p(\lambda) + J_{W_d}(\lambda) + J_{p,x_4}^{+}(\lambda) + J_{W_b,x_4}(\lambda)}{qF(\lambda)\left(1 - R(\lambda)\right)} \tag{13}$$

Hence the photocurrent density supplied by the proposed cell is measured as [24].

$$J_{ph} = \int_0^\infty qF(\lambda)[1 - R(\lambda)]SR(\lambda)d\lambda \tag{14}$$

3. Results and Discussion

The high-low factor has been calculated from equation (7), whereas the spectral response and the photocurrent density have been calculated using equation (13) and (14) respectively. Wavelength of the incident photons used for the calculation of photocurrent density has been ranged from 0.24 μm to 1.08 μm, and photon density corresponding to different wavelengths has been measured following the relation as proposed by Liou and Wang [29] for this simulation. α as a function of λ has been measured by the relation discussed in [30]. Effect of heavy doping in narrowing band gap has been considered and doping dependent mobilitites, diffusion coefficients and minority carrier lifetime have been taken into account.

Graphical representation of the high-low factor against acceptor concentration N_a^+ for various values of front surface recombination velocity (S_n) is shown in Fig. 2. The high-low factor increases as the value of S_n decreases and also as the acceptor concentration in the p^+ layer is increased. On the other hand high-low factor decreases for increasing values of S_n. At higher values of the recombination velocity more and more carriers are lost, giving low values of high-low factor.

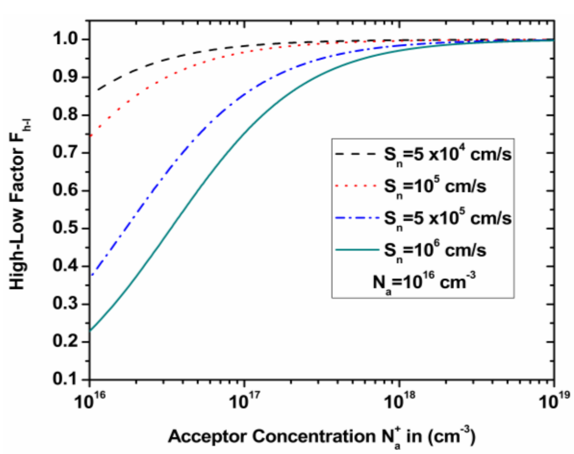

Fig. 2. High-low factor with acceptor concentration.

The variation of SR as a function of wavelength of incident photons is shown in Fig. 3 for various values of acceptor density N_a^+. The value of N_a is chosen as $10^{16}\,cm^{-3}$ for this graph. For a particular value of N_a^+, if wavelength of the incident photons gradually increases, spectral response increases slowly and attains maximum value, and then if the wavelength is further increased, spectral response abruptly falls. On the other hand as the value of N_a^+ increases, spectral response increases due to increased values of high-low factor at the front.

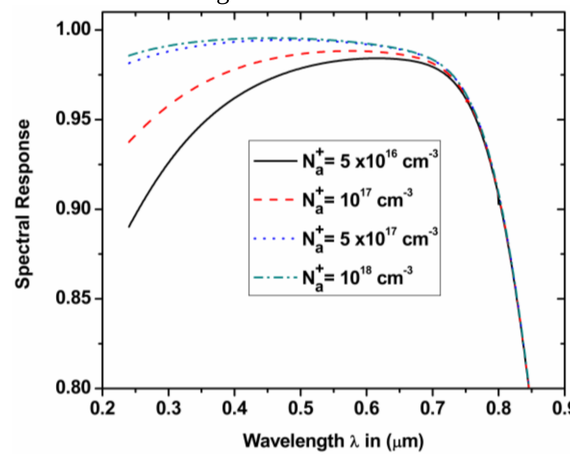

Fig. 3. Spectral response (SR) against wavelength of incident photons.

Photocurrent density versus front layer width W_{p^+} is plotted in Fig. 4 for various values of acceptor concentration N_a^+. It is observed that for a particular value of N_a^+, photocurrent density almost remains constant as W_{p^+} increases, whereas photocurrent increases significantly when N_a^+ is increased.

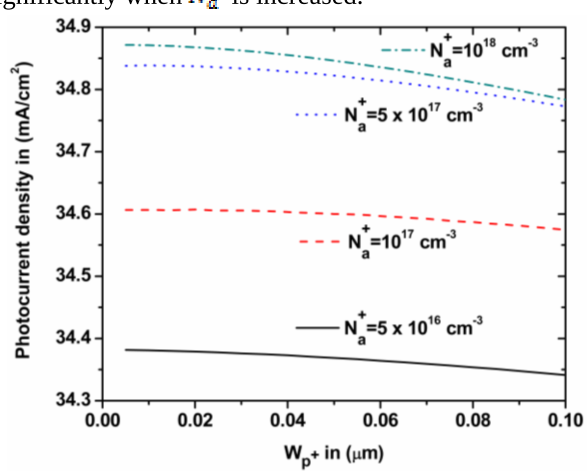

Fig. 4. Photocurrent density against W_p^+.

The variation of photocurrent density with W_p is shown in Fig. 5 for various values of acceptor concentration N_a. It is noticed that for a particular value of N_a, photocurrent density decreases as the value of W_p is increased. The photocurrent density decreases for increasing values of N_a. This may be explained following the argument that the effective surface recombination velocity in p region increases when N_a increases and hence photocurrent decreases due to carrier lost at high recombination.

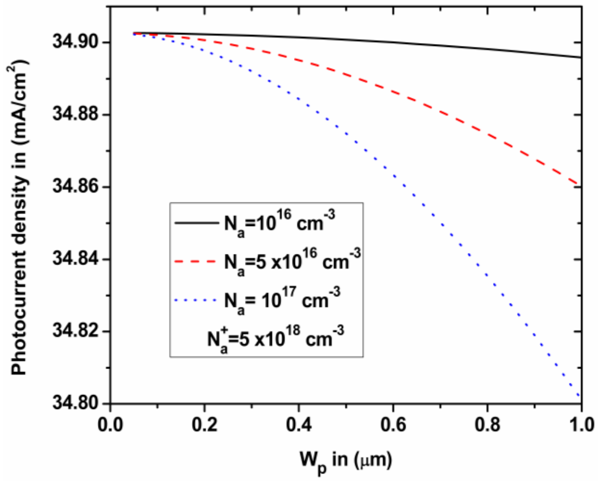

Fig. 5. Photocurrent density with W_p for different values of N_a.

The calculated photocurrent density for various types of silicon solar cells has been graphically shown in Fig. 6 for increasing values of the concerned cell thickness. Solid curve represents the photocurrent density (J_{ph}) for a normal p-n junction device whereas dotted curve represents that of a FSF solar cell, and dashed curve corresponds to J_{ph} for a BSF cell and dashed with dotted curve gives the photocurrent density of the proposed p^+ p n n^+ device in which both front –surface- field and back -surface -field are present. This is observed from the figure 6 that the photocurrent density of the proposed solar cell is not only larger than the normal p-n junction and FSF solar cells but also this is slightly higher than p^+ n n^+ BSF cell. This is because this proposed structure includes the effects of both the front and the back surface fields.

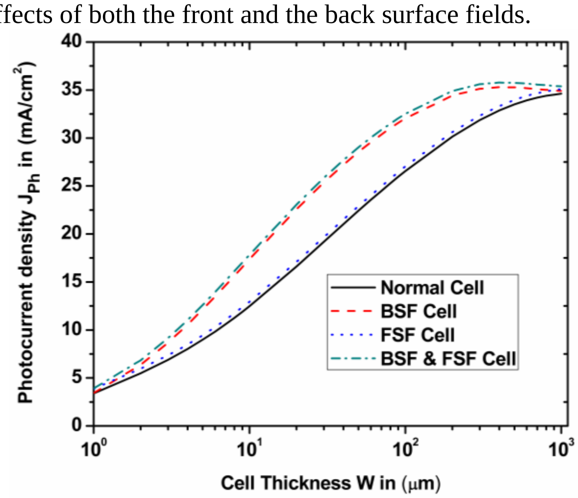

Fig. 6. Photocurrent density versus cell thickness for various types of solar cells.

The calculations carried out on the basis of the analysis derived in this paper give some optimum values of the cell parameters for giving improved performance. These parameters are given in Table 1.

Table 1. The optimized parameters for the proposed p^+ p n n^+ device.

$W_{p^+} = 0.05\ \mu m,\ W_p = 0.5\ \mu m,$

$N_a^+ = 5\times10^{18}\ cm^{-3}, N_a = 2\times10^{17} cm^{-3},$

$W_{n^+} = 0.1\ \mu m, W = 180\ \mu m,$

$N_d = 1\times10^{15} cm^{-3},\ N_d^+ = 5\times10^{18}\ cm^{-3}$

Calculated photocurrent density $J_{ph}(mA/cm^2)$ for various solar cells.

Normal	BSF	FSF	BSF & FSF
34.52	35.67	34.78	35.93

Suggestions for future work:

(i) This work may be suitable for designing silicon solar cells having improved performance and further experimental investigation may be carried in this direction.

(ii) Some extension of this work may be carried out by considering the materials such as GaAs and InAs.

4. Conclusion

In this paper the photocurrent and spectral response of a proposed p^+ p n n^+ device have been investigated analytically and the importance of low-high junction in improving photocurrent has been discussed. Basically the contribution of the p^+p junction is the remarkable reduction of the surface recombination velocity in p-region, which enhances the photocurrent contribution from the p-layer. Theoretically, unit value of F_{h-l} implies the best carrier collection of the low-high junction. However, the experimental values will be always less than this. The most significant contribution of this work is to simultaneously consider the effects of both front-surface-field and back-surface-field in the operation of a solar cell. It is concluded from the present work that spectral response and photocurrent are significantly higher for p^+ p n n^+ structure, as compared to the case when a normal p n n^+ structure is considered.

Acknowledgement

We express our thanks to IACS Kolkata, whose Library we consulted frequently.

References

[1] D. M. Chapin, C. S. Fuller and G. L. Pearson, "A new silicon p-n junction photocell for converting solar radiation into electrical power", *J. Appl. Phys.*, vol. 25, pp. 676-677, 1954.

[2] V. Aroutiounian, S. Petrosyan, A. Khachatryan and K. Touryan, "Quantum dot solar cells", *J. Appl. Phys.*, vol. 89, pp. 2268-2271, 2001.

[3] S. Biswas, A. Chatterjee, A. K. Biswas and A. Sinha, "Spectral response of the intrinsic region of a GaAs–InAs quantum dot solar cell considering the absorption spectra of ideal cubic dots", *Physica E*, vol. 84, pp. 108-111, 2016.

[4] K. W. J. Barnham and G. Duggan, "A new approach to high-efficiency multi-band-gap solar cells", *J. Appl. Phys.*, vol. 67, pp. 3490-3493, 1990.

[5] J. Nelson, M. Paxman, K. W. J. Barnham, J. S. Roberts and C. Button, "Steady-state carrier escape from single quantum wells", *IEEE J. Quantum Electronics*, vol. 29, pp. 1460-1468, 1993.

[6] A. Chatterjee, A. K. Biswas and A. Sinha, "An analytical study of the various current components of an AlGaAs / GaAs multiple quantum well solar cell", *Physica E*, vol. 72, pp. 128-133, 2015.

[7] Dilan ALP, "Quantum photovoltaic effect: Two photon process in solar cell", International Conference on *Renewable Energy Research and Applications (ICRERA)*, Palermo, Italy, pp. 1084-1088, 22-25 November 2015.

[8] M. A. Humayun et al., "Improvement of Temperature Dependence of Carrier Characteristics of Quantum Dot Solar Cell Using InN quantum dot",IJRER, Vol.7, No.1, 2017.

[9] S. Biswas and A. Sinha, "An analytical study of the minority carrier distribution and photocurrent of a p-i-n quantum dot solar cell based on the InAs/GaAs system", *Indian J Phys*, vol. 91, no. 10, pp. 1197-1203, 2017.

[10] Sun Y., Yan X., Yuan C., Luo H. and Jiang Q., "The I-V characteristics of solar cell under the marine environment: Experimental research, International Conference on *Renewable Energy Research and Applications (ICRERA)*, Palermo, Italy, pp. 403-407, 22-25 November 2015.

[11] Zhang Y., Sun Y., Luo H. and Wang Y., "Study on effect of ship low frequency vibration on the output characteristics of PV cells under different solar irradiation", International Conference on *Renewable Energy Research and Applications (ICRERA)*, Palermo, Italy, pp. 388-392, 22-25 November 2015.

[12] Ahamed Md T., Goncalves T., and Tlemcani M, "Single diode model parameters analysis of photovoltaic cell", International Conference on *Renewable Energy Research and Applications (ICRERA)*, Birmingham, UK, pp. 396-400, 20-23 November 2016.

[13] Dida A.H., and Bekhti M, "Study, modeling and simulation of the electric characteristic of space satellite solar cells", International Conference on *Renewable Energy Research and Applications (ICRERA)*, San Diego, CA, USA, pp. 983-987, 5-8 November 2017.

[14] J. Mandelkorn and J. L. Lamneck, "A new electric field effect in silicon solar cell", *J. Appl. Phys.*, vol. 44, pp. 4785-4787, 1973.

[15] A. Sinha and S. K. Chattopadhyaya, "Effect of heavy doping on the properties of high-low junction", *IEEE Transactions on Electron Devices*, vol. 25, pp. 1412-1414, 1978.

[16] J. Dell Alamo et al, "High-low junctions for solar cell applications", *Solid State Electronics* vol. 24, pp. 533-538, 1981.

[17] C. T. Sah, F. A. Lindholm and J. G. Fossum, "A high-low junction emitter structure for improving silicon solar cell efficiency", *IEEE Transaction on Electron Devices*, vol. 25 (1), pp. 66-67, 1978.

[18] Oldwig Ven Roos, "The spectral response of a front surface field solar cell", J. Appl. Phys., vol. 51, pp. 1852, 1980.

[19] A. Zouari and A. B. Arab, "Effect of the front surface field on crystalline silicon solar cell efficiency", Renewable Energy, vol. 36, no. 6, pp. 1663-1670, 2011.

[20] X. M. Dai and Y. M. Tang, "A simple general analytical solution for the quantum efficiency of front-surface-field solar cells", *Solar Energy Materials and Solar cells*, vol. 43, pp. 363-376, 1996.

[21] A. Belghachi and A. Helmaoui, "Effect of the front surface field on GaAs solar cell photocurrent", *Solar Energy Materials and Solar cells*, vol. 92, pp. 667-672, 2008.

[22] A. Ibrahim, "Dark current-Voltage characteristics and Lock-in Thermography Technique as Diagnostic Tools for Monocrystalline Silicon Solar cells", *International Journal of Renewable Energy Research*, vol. 1, no. 3, pp. 60-65, 2011.

[23] A. Sinha et al., "The Injected Dark Current of a p^+ n and a p^+ n n^+ Silicon Solar Cell Taking into Account the Narrowing of Band Gap Due to Heavy Doping", *International Journal of Renewable Energy Research*, vol.6, no.1, pp. 10-14, 2016.

[24] H. J. Hovel, *Semiconductors and Semimetals* vol.11 Solar cells, New York: Academic Press, 1975, pp. 16-20 and 37-38.

[25] J. R. Hauser and M.A. Littlejohn, "Approximations for accumulation and inversion space charge layers in semiconductors", *Solid State Electron*, vol. 11, pp. 667-674, 1968.

[26] A. K. Biswas, A. Chatterjee and A. Sinha, "The minority carrier profile in the front region of a p^+ n junction silicon solar cell and its contribution to spectral response", *Journal of Electron Devices*, vol. 20, pp. 1772-1776, 2014.

[27] A. K. Biswas, A. Chatterjee, S. Biswas and A. Sinha, "Minority carrier distribution in the base region of a p^+ n junction silicon solar cell and its contribution to the spectral response", *International Journal of Renewable Energy Research,* vol. 4 no. 3, pp. 791-794, 2014.

[28] S. M. Sze and K. K. Ng, *Physics of Semiconductor Devices*, John Wiley and Sons, 2007, pp 80-83.

[29] J. J. Liou and W. W. Wong, "Comparison and optimization of the performance of Si and GaAs solar cells", *Solar Energy Materials and Solar Cells*, vol. 28, pp. 9-28, 1992.

[30] E. Fred Schubert, *Light Emitting Diodes*, 2nd edition, Cambridge University Press, 2003, pp.115, 307.

Nomenclature:

p^+ heavily donor doped region
p lightly donor doped region
n^+ heavily acceptor doped region
n lightly acceptor doped region
W_{p^+} width of p^+ type region
W_p width of p type region
W_{n^+} width of n^+ type region
W_n width of n type region
W_a depletion region width produced at high-low junction
W_d depletion region width produced at p-n junction
W_b depletion region width produced at low-high junction
W thickness of the entire solar cell
$(\Delta n)_{p^+}$ excess minority carrier (electron) concentration in p^+ type region
Δn_o excess minority carrier (electron) concentration at high-low junction
S_n front surface recombination velocity for electron
D_n^+ diffusion coefficient for electrons in p^+ type region
L_n^+ diffusion length of electrons in p^+ type region
q electronic charge
λ wavelength of incident photons
$\alpha(\lambda)$ absorption coefficient of the material of solar cell
$F(\lambda)$ incident photon density
$R(\lambda)$ reflection coefficient of the material of solar cell
Γ a factor shown in the text
$J^+_{n,x_1}(\lambda)$ electron photocurrent density contributed from p^+ type region
$J^o_{n,x_1}(\lambda)$ electron photocurrent density collected at high-low junction
S_{e,pp^+} effective surface recombination velocity of electrons in p layer due to the influence of electrons in p^+ region
S_{e,p^+p} effective surface recombination velocity of electrons in p^+ layer due to the influence of electrons in p region
S_{e,nn^+} effective surface recombination velocity of holes in n layer due to the influence of holes in n^+ region
S_{e,n^+n} effective surface recombination velocity of holes in n^+ layer due to the influence of holes in n region
N_a^+ acceptor concentration in p^+ region
N_a acceptor concentration in p region

N_{aeff}^{+} effective acceptor concentration in p^+ region

N_{aeff} effective acceptor concentration in p region

F_{h-l} high-low factor

$J_{W_a,x_3}(\lambda)$ photocurrent density collected at x_3 on account of (p^+ p) high-low junction

D_n diffusion coefficient of electrons in p type region

L_n diffusion length of electrons in p type region

D_p diffusion coefficient of holes in n type region

L_p diffusion length of holes in n type region

$J_n(\lambda)$ electron photocurrent density contributed from p type layer

$J_p(\lambda)$ hole photocurrent density contributed from n type layer

$J_{W_d}(\lambda)$ photocurrent density contributed from p-n junction deletion layer

$J_{p,x_4}^{+}(\lambda)$ hole photocurrent density contributed from n^+ type layer and collected at x_4

$J_{W_b,x_4}(\lambda)$ hole photocurrent density contributed from n type layer and collected at x_4

$SR(\lambda)$ spectral response of the solar cell

J_{Ph} total photocurrent density obtained from the solar cell